

Poly(styrene-*b*-tetrahydrofuran)/Clay Nanocomposites by Mechanistic Transformation

ZULEYHA YENICE,¹ M. ATILLA TASDELEN,² AYHAN ORAL,³ CETIN GULER,¹ YUSUF YAGCI²

¹Department of Chemistry, Ege University, 35100 Bornova, Izmir, Turkey

²Department of Chemistry, Istanbul Technical University, 34469 Maslak, Istanbul, Turkey

³Department of Chemistry, Canakkale Onsekiz Mart University, 17020 Canakkale, Turkey

Received 12 December 2008; accepted 31 January 2009

DOI: 10.1002/pola.23332

Published online in Wiley InterScience (www.interscience.wiley.com).

ABSTRACT: Synthesis of poly(styrene-*block*-tetrahydrofuran) (PSt-*b*-PTHF) block copolymer on the surfaces of intercalated and exfoliated silicate (clay) layers by mechanistic transformation was described. First, the polystyrene/montmorillonite (PSt/MMT) nanocomposite was synthesized by *in situ* atom transfer radical polymerization (ATRP) from initiator moieties immobilized within the silicate galleries of the clay particles. Transmission electron microscopy (TEM) analysis showed the existence of both intercalated and exfoliated structures in the nanocomposite. Then, the PSt-*b*-PTHF/MMT nanocomposite was prepared by mechanistic transformation from ATRP to cationic ring opening polymerization (CROP). The TGA thermogram of the PSt-*b*-PTHF/MMT nanocomposite has two decomposition stages corresponding to PTHF and PSt segments. All nanocomposites exhibit enhanced thermal stabilities compared with the virgin polymer segments. © 2009 Wiley Periodicals, Inc. *J Polym Sci Part A: Polym Chem* 47: 2190–2197, 2009

Keywords: atom transfer radical polymerization (ATRP); block copolymers; cationic polymerization; cationic ring opening polymerization; clay; mechanistic transformation; nanocomposites

INTRODUCTION

There has been intense interest in the preparation of polymer/clay nanocomposites over the last decade as a result of improvements in many physical properties, such as flame retardancy, high dimensional stability, and mechanical strength when compared with the pure polymer or conventional composite materials with microscale structure.^{1–3} Two idealized structures of the polymer/clay composites can be achieved: intercalated and exfoliated structures. These are contingent upon

the distribution and ordering of the clay particles or layers in the polymer matrix. The exfoliated structure is obtained when the individual silicate layers are fully dispersed in a polymer matrix with nanoscopic dimensions. Often, the silicate layers are not completely exfoliated and are better described either as intercalated or as both. There are several methods to synthesize polymer/clay nanocomposites: solution exfoliation, melt intercalation, and *in situ* intercalative polymerization.⁴ In the *in situ* intercalative polymerization technique, the silicate layers are swollen within the monomer solution. The polymerization happens between the intercalated layers and is initiated either thermally or chemically *in situ*. Various *in situ* polymerization methods for preparing

Correspondence to: Y. Yagci (E-mail: yusuf@itu.edu.tr)

Journal of Polymer Science: Part A: Polymer Chemistry, Vol. 47, 2190–2197 (2009)
© 2009 Wiley Periodicals, Inc.

polymer/clay nanocomposites are reported. These include ring-opening polymerization (ROP),^{5–8} controlled radical polymerization (CRP),^{8–20} conventional free radical polymerization,^{21–27} cationic polymerization,^{26,28,29} and living anionic polymerization.³⁰

Although most of the efforts have been concentrated on homopolymers, there is also interest in block copolymer silicate nanocomposites because of their higher complex structure and technological significance. However, there are few reports on *in situ* preparation of block copolymer silicate nanocomposites^{8,11,12,31,32} such as: poly(styrene-*b*-butyl acrylate)/silicate nanocomposite^{11,12} by *in situ* sequential atom transfer radical polymerization (ATRP)^{33–35} from initiators immobilized within the silicate galleries of the clay particles and poly(styrene-*b*-caprolactone)/silicate nanocomposite⁸ by nitroxide mediated polymerization (NMP) and ROP process from a silicate anchored bifunctional initiator concurrently.

Mechanistic transformation provides a facile route to synthesis of block copolymers that cannot be made by a single polymerization mode.^{36–40} In this concept, a polymer, obtained by a particular polymerization mechanism, is functionalized either by initiation or termination steps.^{41–44} The polymer is isolated and purified, and finally, the functional groups are converted into another kind of species capable of initiating the polymerization of the second monomer.^{45,46} A wide range of combinations of different polymerization modes has been reported and recently reviewed.⁴⁰

In this article, we report a transformation approach for the synthesis of (PSt-*b*-PTHF)/MMT nanocomposite involving a mechanistic change from ATRP to cationic ring opening polymerization (CROP).⁴³ The resulting exfoliated polymer/clay nanocomposites have been characterized by X-ray diffraction (XRD) spectroscopy, thermogravimetric analysis (TGA), and transmission electron microscopy (TEM).

EXPERIMENTAL

Materials

Montmorillonite (MMT) was kindly donated by Sud Chemie [Nanofil 116, cationic (Na⁺) exchange capacity of 100 meq/100 g]. Styrene (St; 99%, Aldrich) was passed through basic alumina column to remove the inhibitor. Tetrahydrofuran (THF; HPLC grade, Aldrich) was dried on sodium wire under reflux in the presence of traces of ben-

zophenone until a blue color persisted and was used directly after distillation. *N,N,N',N''*,*N'''* pentamethyldiethylene triamine (PMDETA; 99%, Aldrich), used as a ligand, was distilled before use. Silver hexafluorophosphate (AgPF₆; 98%, Acros), copper bromide (CuBr; 98%, Acros), 6-amino-1-hexanol (97%, Acros), 2-bromoisobutyl bromide (98%, Aldrich), hydrochloric acid (HCl; 37% ACS reagent, Aldrich), and sodium chloride (NaCl, 98%, Acros) were used as received. Other solvents were purified by conventional drying and distillation procedures.

Synthesis of 6-[(2-bromo-2-methylpropanoyl)oxy]hexan-1-Ammonium Chloride

For this purpose, first the quaternization of the amine group of 6-amino-1-hexanol was performed. Thus, 1.5 g 6-amino-1-hexanol (14.6 mmol) was dissolved in 6 mL CH₂Cl₂ in a schlenk flask under argon atmosphere. Saturated HCl/diethyl ether solution (30 mL) was added drop wise to the solution, and the mixture was stirred for 3 h. After evaporation, the yellowish product (6-hydroxy hexan-1-ammonium chloride) was obtained. Then, it was dried *in vacuo* at ambient temperature for 24 h.

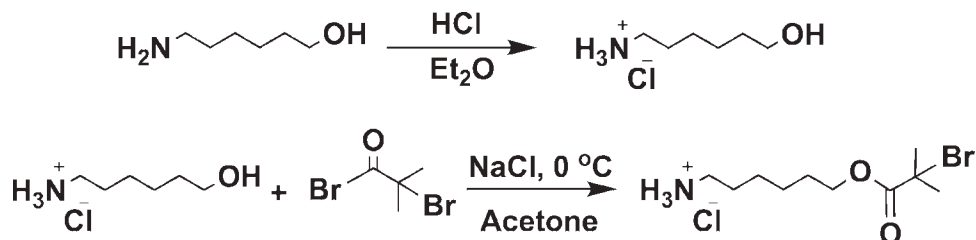
In the second part, the esterification of 6-hydroxy hexan-1-ammonium chloride with 2-bromo-isobutyryl bromide was performed. 6-hydroxy hexan-1-ammonium chloride (1.4 g, 13.7 mmol) was dissolved in 10 mL anhydrous acetone into a balloon and was cooled in an ice bath. A solution of 2-bromoisobutyryl bromide (1.7 mL, 13.7 mmol) dissolved in 10 mL anhydrous acetone was added drop wise into a balloon. After stirring the mixture for 20 h, the solvent was evaporated. The final product was precipitated in cold diethyl ether and filtered. Then, it was dried *in vacuo* at ambient temperature for 24 h (70% yields).

The initiator's ¹H NMR data were represented as below:

¹H NMR (CDCl₃, 300 MHz) 7.978 [s, 3H, NH₃], 4.178 (t, 2H, CH₂O), 3.075 (m, 2H, CH₂N), 1.79 [s, 6H, (CH₃)₂], 1.744 (m, 2H, CH₂), 1.726 (quintet, 2H, CH₂), 1.677 [m, 4H, (CH₂)₂]

Preparation of the ATRP Initiator/MMT (O-MMT)

Modification of the clay was carried out according to described procedure.¹⁸ The initiator was ion-exchanged onto MMT. The initiator (1000 mg) and montmorillonite clay (2500 mg) was added into 50 mL of acetone, and the mixture was



Scheme 1. Synthesis of 6-[(2-bromo-2-methylpropanoyl)oxy]hexan-1-ammonium chloride.

stirred overnight. The solids were filtered and washed with acetone than dried *in vacuo*, at room temperature (organic content of organomodified clay was found to be around 17 wt % as calculated by TGA).

Synthesis of Polystyrene/Clay Nanocomposite via ATRP

The above obtained organomodified montmorillonite (O-MMT, 250 mg, 0.174 mmol (organic content), monomer (St, 2 mL, 17.4 mmol), CuBr (17 mg, 0.174 mmol), and PMDETA (0.021 mL, 0.174 mmol) were added to the flask. The reaction mixture was degassed by three freeze-pump-thaw cycles and left *in vacuo*. The tube was then placed in a stirrer at 110 °C for given time. The mixture was precipitated in methanol, and the precipitated polymer was filtered off and dried *in vacuo*. To remove the copper contaminants from the nanocomposite, the product was washed thoroughly with aqueous solution of disodiumsalt-ethylenediamine tetraacetic acid (EDTA) to remove the catalysts,⁴⁷ then with water and dried in vacuum at 40 °C.

Synthesis of Polystyrene-*b*-Polytetrahydrofuran/Clay Nanocomposite via CROP

The block copolymer/MMT nanocomposite was prepared by the CROP of THF with PSt/MMT in combination with silver hexafluorophosphate as the initiator. A typical procedure was as follows: precursor PSt/MMT-1 (400 mg, 0.03 mmol), silver hexafluorophosphate (~26 mg, 0.1 mmol), and THF (10 mL, 122 mmol) were added to three-necked, round-bottomed flask under a nitrogen atmosphere in an ice bath. The reaction was brought to 20 °C and stirred for 16 or 24 h. After a given time, the polymerization was stopped by

the addition of a small amount of methanol. The polymer was then precipitated in cold pentane (−20 °C), filtered off on a cold glass filter, and finally dried *in vacuo*.

Characterization

Gel permeation chromatography (GPC) measurements were obtained from a Viscotek GPCmax Autosampler system consisting of a pump, three ViscoGEL GPC columns (G2000_{HHR}, G3000_{HHR} and G4000_{HHR}), a Viscotek UV detector, and Viscotek a differential refractive index (RI) detector with a THF flow rate of 1.0 mL min^{−1} at 30 °C. Both detectors were calibrated with PS standards having narrow molecular weight distribution. Data were analyzed using Viscotek OmniSEC Omni-01 software. ¹H NMR spectra in CDCl₃ with Si(CH₃)₄ as an internal standard were recorded at room temperature at 250 MHz using a Bruker DPX 250 spectrometer. For GPC and ¹H NMR measurements, the polymers were cleaved from clay through the refluxing, for about 24 h, of the nanocomposite in THF of LiBr (ca. 5 wt %), followed by centrifugation and filtration through a 0.2 μm filter. Thermal gravimetric analysis (TGA) was performed on Perkin-Elmer Diamond TA/TGA with a heating rate of 10 °C min under nitrogen flow. X-ray diffraction (XRD) patterns were obtained with a Siemens D5000 θ/θ diffractometer equipped with an intrinsic germanium detector system with Cu Kα radiation (λ: 1.54 Å). TEM micrographs analyses were performed with a G2 Spirit BioTwin (FEI Company Tecnai) transmission electron microscope by using an accelerating voltage of 120 kV and 11 Mega pixels Morada Camera. The samples have been dispersed in chloroform and then, some drops were deposed on a carbon supporting grid. After solvent evaporation, the TEM micrograph analyses were performed.

Table 1. XRD Data for Clays and Nanocomposites

Clays and Nanocomposites	d_{001} of Clay (nm)
NaMMT	1.62
O-MMT	2.27
PSt/MMT-1 ^a	No reflection
PSt- <i>b</i> -PTHF/MMT-1 ^b	0.46 and 0.38

^aNanocomposite containing 14% clay content.^bNanocomposite containing 0.8% clay content.

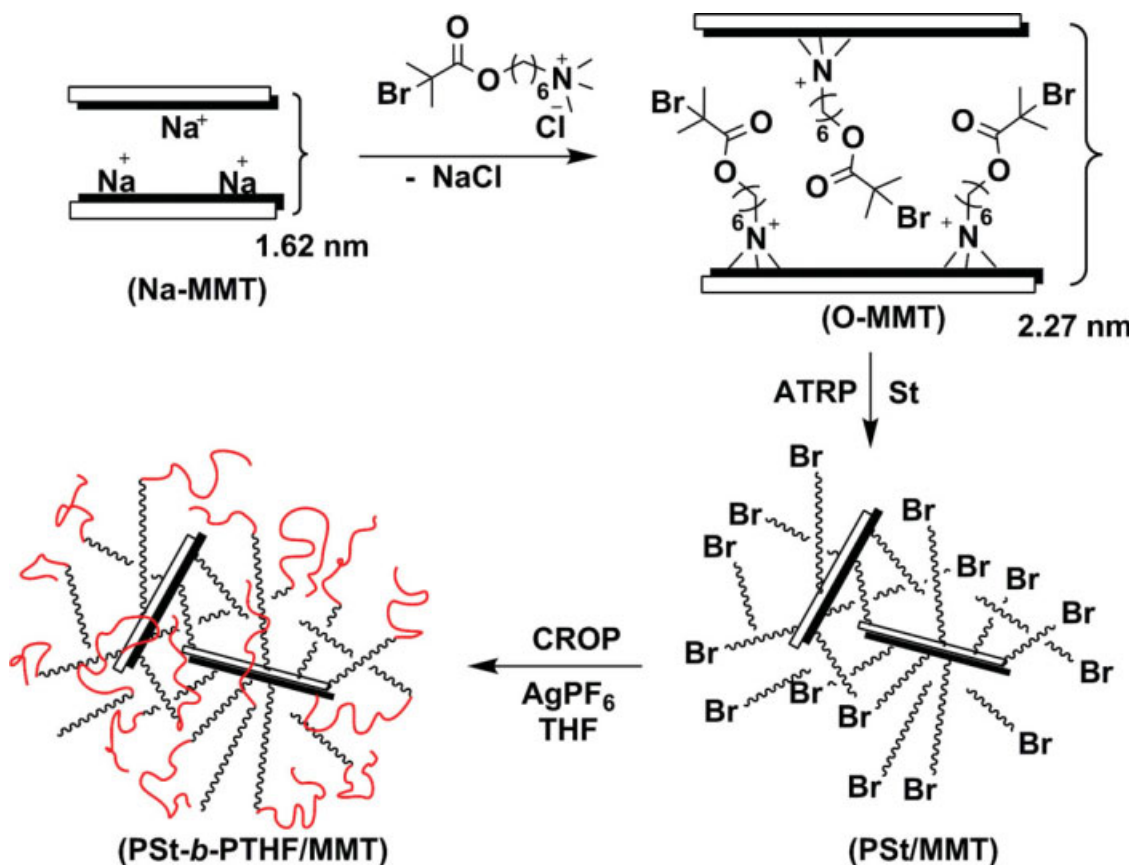
RESULTS AND DISCUSSION

Our synthetic strategy is based on designing a molecule possessing both intercalation and initiator functionalities to be used for ATRP. It was synthesized in a two-step procedure according to Zhao et al.¹⁸ It seemed appropriate to quaternize 6-amino-1-hexanol simply by reacting with HCl to obtain 6-hydroxy hexan-1-ammonium chloride. In the second step, the esterification of quaternized salt with 2-bromo-isobutyryl bromide was per-

formed (Scheme 1). The structure of the resulting quaternized salt, 6-[(2-bromo-2-methylpropanoyl)oxy] hexan-1-ammonium chloride was confirmed by spectral analysis (see Experimental Section).

TGA of the original MMT was found to have 4 wt % volatile materials, with most of the organics decomposing around 200–300 °C. On intercalation with quaternized initiator, the organomodified MMT (O-MMT) clay was analyzed and found to have 21 wt % volatile materials present, and so ~17 wt % of O-MMT was the quaternized initiator. XRD analysis (Table 1) shows that the intercalation of quaternized was successful. The d_{001} spacing of layers was increased by ~0.65 nm, from 1.62 nm in the virgin MMT to 2.27 nm in O-MMT.

ATRP of styrene initiated by O-MMT (Scheme 2) was carried out under various conditions typical for such polymerizations. The molecular weight results and reactions conditions are summarized in Table 2. These show that living radical polymerization through ATRP was successful, with the molecular weight distributions being



Scheme 2. Schematic representation of synthesis of PSt-*b*-PTHF/clay nanocomposites by combination of ATRP and CROP process. [Color figure can be viewed in the online issue, which is available at www.interscience.wiley.com.]

Table 2. Synthesis of Polystyrene/Montmorillonite Nanocomposites by *In Situ* ATRP at 110 °C

Code	Molar Ratio ^a	Time (h)	Yield (%) ^b	M_n^c	M_w/M_n^c
PSt/MMT-1 ^d	1/100/1/1	3	17	11,600	1.37
PSt/MMT-2 ^d	1/100/1/1	5	28	22,000	1.27
PSt/MMT-3 ^e	1/100/1/1	3	57	36,000	1.51
PSt/MMT-4 ^d	1/200/1/1	3	11	12,000	1.39
PSt/MMT-5 ^d	1/200/1/1	5	21	39,000	1.36

^a [Initiator]/[St]/[CuBr]/[Ligand].

^b Determined by gravimetric analysis.

^c Determined by GPC.

^d In toluene.

^e In bulk.

relatively narrow polydispersity ($M_w/M_n < 1.51$), under a variety of experimental conditions. It should also be pointed out that the homopolymer nanocomposite, namely PSt/MMT-1, displays an exfoliated structure as confirmed by the absence of any d_{001} reflection in the XRD region (see Table 1).

The PSt/MMT nanocomposites obtained by ATRP have been analyzed by TEM (Fig. 1). Thin clay nanoplatelets proved randomly distributed in the PSt matrix, as shown by finely dispersed nanolayers as observed from their edge side [Fig. 1(A)]. However, as far as the composites pre-

pared by *in situ* polymerization are concerned, although the absence of aggregates confirms the high degree of exfoliation of the layered silicates, some small intercalated stacks with a thickness of a few tenths of nanometers remain from time to time as observed on Figure 1(B). This may be due to the incomplete activation of initiator and although at limited rate, some transfer reactions occurred during the *in situ* polymerization.¹⁸

The block copolymer/clay nanocomposites were prepared by the CROP of THF with PSt/MMT in combination with silver hexafluorophosphate as the initiator. It is known that PSt obtained by

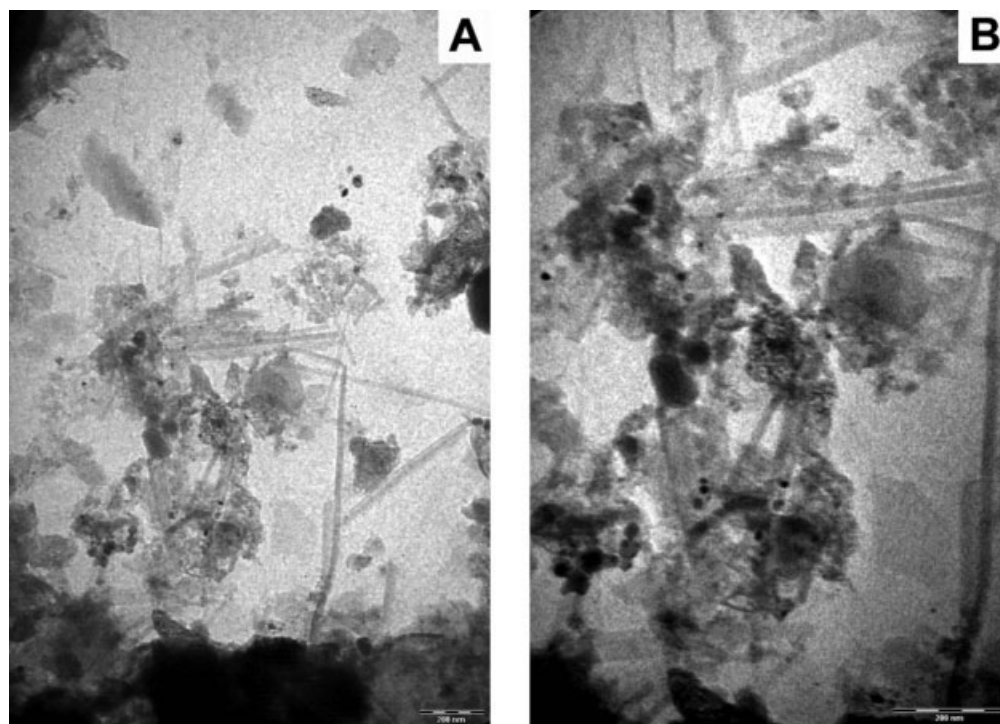


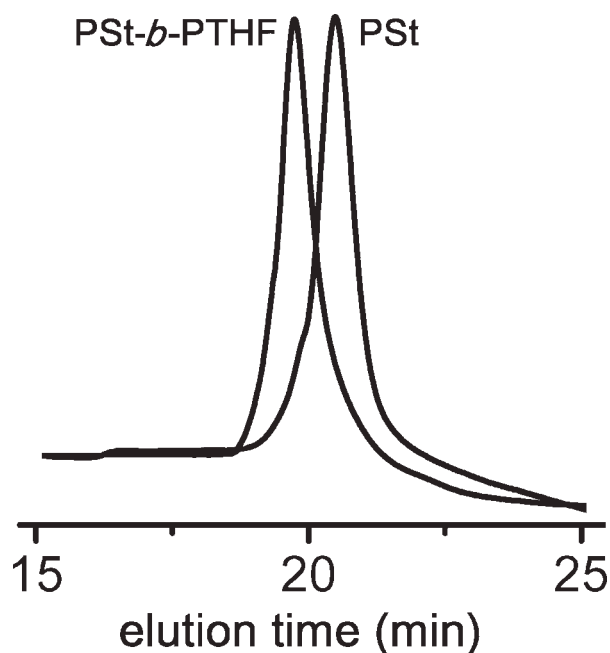
Figure 1. TEM micrographs of PS/MTT nanocomposites; exfoliated (A) and intercalated (B) structures.

Table 3. Synthesis of Polystyrene-*b*-Polytetrahydrofuran/Montmorillonite Nanocomposites by CROP at 0 °C

Code	Molar Ratio ^a	Time (h)	Yield (%) ^b	M_n^c	M_w/M_n^c	Composition ^d	
						St	THF
PSt- <i>b</i> -PTHF/MMT-1 ^e	0.03/0.1/122	16	14	13,900	1.41	83	17
PSt- <i>b</i> -PTHF/MMT-2 ^e	0.06/0.2/122	16	17	16,800	1.40	69	31
PSt- <i>b</i> -PTHF/MMT-3 ^f	0.03/0.1/122	24	22	17,100	1.58	70	30
PSt- <i>b</i> -PTHF/MMT-4 ^f	0.06/0.2/122	24	26	19,000	1.64	63	37

^a [PSt/MMT]/[AgPF₆]/[THF].^b Determined by gravimetric analysis.^c Determined by GPC.^d Calculated from ¹H NMR spectroscopy.^e Precursor polymer: PSt/MMT-1.^f Precursor polymer: PSt/MMT-4.

ATRP contains terminal halide groups, which can be converted to the initiating carbocations when reacted with silver salts containing non-nucleophilic counter anions. Such counter anions ensues successful chain growth by stabilizing propagating cation. The polymerization conditions and results are listed in Table 3. As we can see from Table 3, after transformation reaction, the elution peaks of block copolymers were shifted to the high molecular weights and molecular weight distributions were broadened slightly (Fig. 2). These results clearly indicate that PSt/MMT nanocomposites that have exfoliated and intercalated structures were successfully used as initiators in

**Figure 2.** GPC curves of homo and block copolymer after separated with LiBr.

conjunction with the silver salt in a manner similar to that described for the bare PSt.⁴³ This process results in the formation of block copolymers within the silicate layers.

The structure of the block copolymer was analyzed by ¹H NMR spectroscopy. A typical spectrum is shown in Figure 3(B). The new peak centered at 3.72 ppm was assigned to the protons of the methylene groups connected to oxygen from the PTHF segment. The disappearance of the peak corresponding to the proton located at the α -position of the chain end at 4.4 ppm [Fig. 3(A)] is additional evidence for the successful block copolymerization.

Figure 4 shows XRD spectra of clay, ATRP initiator modified clay and PSt/clay and PSt-*b*-PTHF/clay nanocomposites. For the PSt/clay nanocomposite, the d_{001} diffraction peak on

XRD spectra disappeared, which implies that the layered structure in the clay particles is largely destroyed by *in situ* ATRP process. PTHF is a crystalline polymer with a planar zigzag conformation.⁴⁸ The crystal structure of PTHF was studied in detail by XRD analysis,^{48,49} and it was shown that the polymer has two diffraction peaks. In our case, after block copolymerization, these characteristic peaks emerged at 0.46 and 0.38 nm.

In Figure 5, TGA thermograms of PSt/MMT and PSt-*b*-PTHF/MMT nanocomposites, prepared by *in situ* ATRP and mechanistic transformation from ATRP to CROP, respectively, are shown. For comparison, thermograms of the precursor compounds were also compiled in the figure. From the TGA data, it is clear that the degradation temperature of the PSt/MMT nanocomposites containing silicate layers shifted toward a higher temperature than those of neat polymers. The

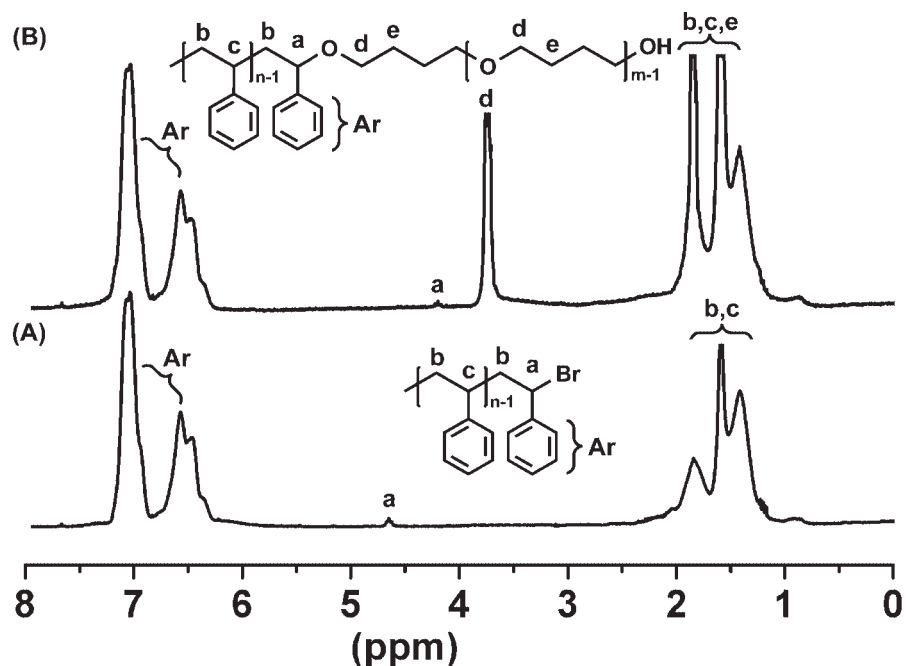


Figure 3. ^1H NMR spectra of PSt (A) and PSt-*b*-PTHF copolymer (B) after separated with LiBr.

thermogram of the PSt-*b*-PTHF/MMT nanocomposite has two decomposition stages. The first one was in 230–320 °C range and the weight loss is about 25% corresponding to PTHF chains. Second one was in 320–440 °C range and the weight loss is about 65% corresponding to PSt chains. These values are in close agreement with the composition of the block copolymer. All nanocomposites exhibit enhanced thermal stabilities compared to the virgin polymer. The improved decomposition

temperature of PTHF compare to PSt segment may be related to some physical interaction of polyether with the Si-O-Si layer. Similar behavior was observed for PTHF/clay nanocomposites prepared by click chemistry and CROP.²⁹

In conclusion, PSt-*b*-PTHF block copolymer silicate nanocomposites were synthesized by combination of ATRP and CROP process in controlled manner and mixtures of exfoliated and intercalated structures were observed. Furthermore, this

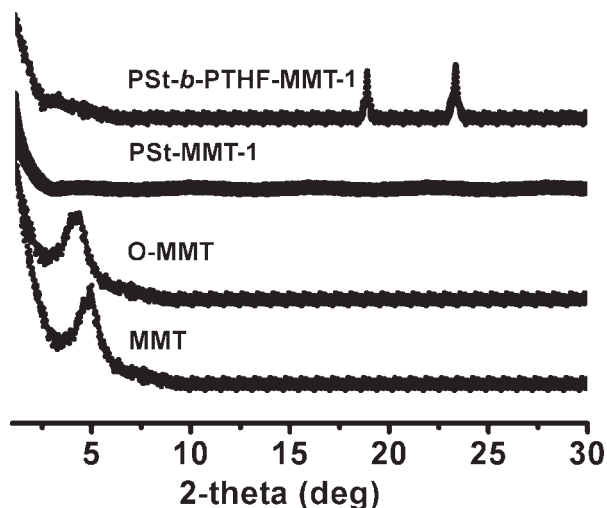


Figure 4. X-ray diffraction curves of clays and nanocomposites.

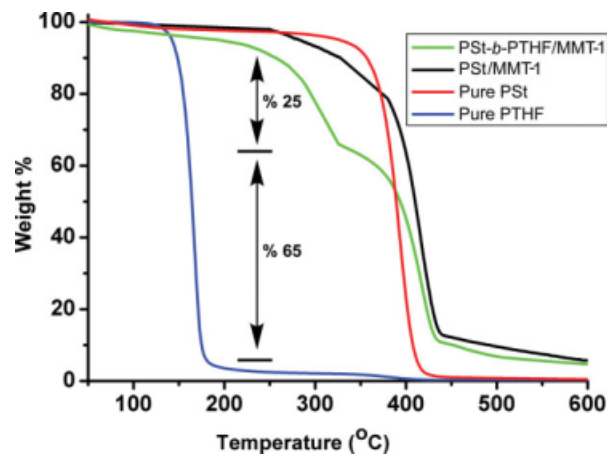


Figure 5. Weight loss for nanocomposites and corresponding compounds; pure PSt, pure PTHF, PSt/MMT-1, and PSt-*b*-PTHF/MMT-1 (see Table 1 for details).

study is the first example of the application of mechanistic transformation for the block copolymer silicate nanocomposites. This type of block copolymer contains soft (PTHF) and hard (PSt) segments and has potential applications as thermoplastic and adhesive materials.

The authors thank Istanbul Technical University, Research Fund for the financial support.

REFERENCES AND NOTES

- Giannelis, E. P. *Adv Mater* 1996, 8, 29–35.
- Okamoto, M. *Mater Sci Tech-Lond* 2006, 22, 756–779.
- Ray, S. S.; Okamoto, M. *Prog Polym Sci* 2003, 28, 1539–1641.
- Alexandre, M.; Dubois, P. *Mater Sci Eng R* 2000, 28, 1–63.
- Kubies, D.; Pantoustier, N.; Dubois, P.; Rulmont, A.; Jerome, R. *Macromolecules* 2002, 35, 3318–3320.
- Lepoittevin, B.; Pantoustier, N.; Devalckenaere, M.; Alexandre, M.; Kubies, D.; Calberg, C.; Jerome, R.; Dubois, P. *Macromolecules* 2002, 35, 8385–8390.
- Viville, P.; Lazzaroni, R.; Pollet, E.; Alexandre, M.; Dubois, P. *J Am Chem Soc* 2004, 126, 9007–9012.
- Di, J. B.; Sogah, D. Y. *Macromolecules* 2006, 39, 5052–5057.
- Di, J. B.; Sogah, D. Y. *Macromolecules* 2006, 39, 1020–1028.
- Weimer, M. W.; Chen, H.; Giannelis, E. P.; Sogah, D. Y. *J Am Chem Soc* 1999, 121, 1615–1616.
- Zhao, H. Y.; Farrell, B. P.; Shipp, D. A. *Polymer* 2004, 45, 4473–4481.
- Zhao, H. Y.; Shipp, D. A. *Chem Mater* 2003, 15, 2693–2695.
- Konn, C.; Morel, F.; Beyou, E.; Chaumont, P.; Bourgeat-Lami, E. *Macromolecules* 2007, 40, 7464–7472.
- Zhang, B. Q.; Pan, C. Y.; Hong, C. Y.; Luan, B.; Shi, P. J. *Macromol Rapid Commun* 2006, 27, 97–102.
- Salem, N.; Shipp, D. A. *Polymer* 2005, 46, 8573–8581.
- Wheeler, P. A.; Wang, J. Z.; Mathias, L. J. *Chem Mater* 2006, 18, 3937–3945.
- Li, C. P.; Huang, C. M.; Hsieh, M. T.; Wei, K. H. *J Polym Sci Polym Chem* 2005, 43, 534–542.
- Zhao, H. Y.; Argoti, S. D.; Farrell, B. P.; Shipp, D. A. *J Polym Sci Polym Chem* 2004, 42, 916–924.
- Bottcher, H.; Hallensleben, M. L.; Nuss, S.; Wurm, H.; Bauer, J.; Behrens, P. *J Mater Chem* 2002, 12, 1351–1354.
- Oral, A.; Shahwan, T.; Guler, C. *J Mater Res* 2008, 23, 3316–3322.
- Tseng, C. R.; Wu, J. Y.; Lee, H. Y.; Chang, F. C. *J Appl Polym Sci* 2002, 85, 1370–1377.
- Fu, X.; Qutubuddin, S. *Polymer* 2001, 42, 807–813.
- Fu, X.; Qutubuddin, S. *Mater Lett* 2000, 42, 12–15.
- Uthirakumar, P.; Song, M. K.; Nah, C.; Lee, Y. S. *Eur Polym Mater* 2005, 41, 211–217.
- Uthirakumar, P.; Nahm, K. S.; Hahn, Y. B.; Lee, Y. S. *Eur Polym J* 2004, 40, 2437–2444.
- Nese, A.; Sen, S.; Tasdelen, M. A.; Nugay, N.; Yagci, Y. *Macromol Chem Phys* 2006, 207, 820–826.
- Akat, H.; Tasdelen, M. A.; Du Prez, F.; Yagci, Y. *Eur Polym J* 2008, 44, 1949–1954.
- Yu, Y. H.; Lin, C. Y.; Yeh, J. M. *J Appl Polym Sci* 2004, 91, 1904–1912.
- Tasdelen, M. A.; Van Camp, W.; Goethals, E.; Dubois, P.; Du Prez, F.; Yagci, Y. *Macromolecules* 2008, 41, 6035–6040.
- Fan, X. W.; Zhou, Q. Y.; Xia, C. J.; Cristofoli, W.; Mays, J.; Advincula, R. *Langmuir* 2002, 18, 4511–4518.
- Pollet, E.; Delcourt, C.; Alexandre, M.; Dubois, P. *Macromol Chem Phys* 2004, 205, 2235–2244.
- Yang, Y. F.; Liu, L.; Zhang, J.; Li, C. X.; Zhao, H. Y. *Langmuir* 2007, 23, 2867–2873.
- Percec, V.; Barboiu, B. *Macromolecules* 1995, 28, 7970–7972.
- Kato, M.; Kamigaito, M.; Sawamoto, M.; Higashimura, T. *Macromolecules* 1995, 28, 1721–1723.
- Wang, J. S.; Matyjaszewski, K. *J Am Chem Soc* 1995, 117, 5614–5615.
- Yagci, Y.; Duz, A. B.; Onen, A. *Polymer* 1997, 38, 2861–2863.
- Hizal, G.; Yagci, Y. *Polymer* 1989, 30, 722–725.
- Yagci, Y.; Serhatli, I. E.; Kubisa, P.; Biedron, T. *Macromolecules* 1993, 26, 2397–2399.
- Hizal, G.; Yagci, Y.; Schnabel, W. *Polymer* 1994, 35, 4443–4448.
- Yagci, Y.; Tasdelen, M. A. *Prog Polym Sci* 2006, 31, 1133–1170.
- Guo, Y. M.; Pan, C. Y.; Wang, J. *J Polym Sci Polym Chem* 2001, 39, 2134–2142.
- Xu, Y. J.; Pan, C. Y. *Macromolecules* 2000, 33, 4750–4756.
- Xu, Y. J.; Pan, C. Y. *J Polym Sci Polym Chem* 2000, 38, 337–344.
- Guo, Y. M.; Pan, C. Y. *Polymer* 2001, 42, 2863–2869.
- Tasdelen, M. A.; Degirmenci, M.; Yagci, Y.; Nuyken, O. *Polym Bull* 2003, 50, 131–138.
- Durmaz, Y. Y.; Karagoz, B.; Bicak, N.; Yagci, Y. *Polym Int* 2008, 57, 1182–1187.
- Sonmez, H. B.; Senkal, B. F.; Sherrington, D. C.; Bicak, N. *React Funct Polym* 2003, 55, 1–8.
- De Witte, I. C.; Goethals, E. *J Polym Adv Technol* 1999, 10, 287–292.
- Cesari, M.; Perego, G.; Mazzei, A. *Makromol Chem* 1965, 83, 196–206.